ISSN: 3007-9640 DOI: https://doi.org/10.70114/acmsr.2025.5.1.P25

Hydrotalcite-Based Composite Photothermal Coupling Catalysts: Realizing Green and Efficient Synthesis of High-Value Hydrogen Peroxide

Qi Wu [1], Liping Guan [1], Xianglong Zhao [1], Wenying Shi [1, 2]

[1] State Key Laboratory of Chemical Resource Engineering, Beijing University of Chemical Technology, Beijing 100029, China;

[2] Quzhou Institute for Innovation in Resource Chemical Engineering, Zhejiang 324000, China.

[a] shiwy@mail.buct.edu.cn

Abstract. In this paper, we intercalated 5,10,15,20-tetra(4-carboxyphenyl)porphine (TCPP) into layered double hydroxides (LDHs), where tilted J-type aggregation extends light absorption to the UV-vis-NIR range and introduces a synergistic photothermal effect. High-energy photons drive electron–hole separation for two-electron O2 reduction to *OOH and H2O2, while low-energy photons generate localized heat to enhance charge separation and lower barriers. The ordered –COOH/–NH groups further adsorb and stabilize *OOH intermediates via hydrogen bonding, enabling efficient and selective H2O2 synthesis under solar light.

Keywords: lamellar double hydroxide; photothermal coupling catalysis; hydrogen peroxide; J-type aggregates.

1. Introduction

Hydrogen peroxide (H_2O_2) is a strategic chemical with both green oxidizing properties and high energy density, and plays an irreplaceable role in paper, textile, semiconductor cleaning, environmental treatment, and new energy. According to market forecasts, global demand for H_2O_2 will increase to approximately 5.7 million tons by 2027, showing strong growth. However, more than 95% of H_2O_2 is still prepared by the traditional anthraquinone (AO) process. This process not only consumes high energy (2200–2500 kWh per ton), but also emits huge carbon emissions, and the core palladium catalyst is highly dependent on imports, which highlights the safety risk of the industrial chain.

Solar-driven photocatalytic direct synthesis of H_2O_2 is considered to be the core pathway to solve the above problems. This method has attracted much attention because it uses H_2O and O_2 as raw materials, the theoretical energy consumption is only 1/10 of that of AO method, and the process is green and environmentally friendly. However, the practical application of photocatalytic technology still faces serious challenges: firstly, the compounding of photogenerated electrons and holes is serious, and the quantum efficiency is generally lower than 1%; secondly, the utilization of traditional catalysts on the solar spectrum is limited to the ultraviolet (UV) and part of the visible light, whereas more than 50% of solar energy is concentrated in the infrared (IR) region, which is not enough to make use of the catalysts; and thirdly, many systems require the addition of sacrificial agents such as isopropanol to inhibit side reactions, which not only limits the continuous operation of the reaction, but also increases the cost and complexity. Thus, to realize the industrial application of photocatalytic synthesis of H_2O_2, it is necessary to make breakthroughs in spectral utilization, carrier separation efficiency, and stability under the condition of no sacrificial agent.

In recent years, layered double hydroxides (LDHs) have become an important platform for the construction of high-performance photocatalysts due to their tunable structure, abundant surface basic sites, and domain-limiting effect of the two-dimensional laminates. The interlayer space of LDHs can effectively restrict the arrangement of organic molecules and induce the formation of highly ordered molecular orientation and π-π stacking pattern, which can improve the charge transport and active site exposure. Meanwhile, the metal composition and charge density of LDHs

ISSN: 3007-9640 DOI: https://doi.org/10.70114/acmsr.2025.5.1.P25
can be finely tuned by adjusting the ratios of Zn, Mg, Ca, Al, etc., which provides rich designability for the photocatalytic process.

Among the organic photocatalytic molecules, porphyrins and their derivatives have been widely investigated for light energy conversion due to their strong light absorption, tunable molecular orientation, and good electron transport properties. Porphyrin stacking critically dictates properties: H-type causes exciton quenching and weak photothermal use, while J-type broadens π-conjugation, boosts NIR absorption, improves charge separation, and enhances photothermal conversion efficiency. This arrangement not only enhances the utilization of 1100–2000 nm low energy light, but also realizes efficient photon-phonon conversion through enhanced intermolecular coupling and produces a localized thermal effect, which significantly improves the photothermal co-catalytic performance.

In this work, 5,10,15,20-Tetra(4-carboxyphenyl)porphine (TCPP) was intercalated into layered double hydroxides (LDHs), enabling tilted molecular alignment to form J-type aggregates, thereby broadening the spectral response across the UV-vis-NIR region and introducing a synergistic photothermal effect. High-energy photons excite electron–hole pairs to drive the two-electron O_2 reduction pathway toward *OOH intermediates and ultimately H_2O_2, while low-energy photons are converted into localized heat through exciton nonradiative relaxation, enhancing charge separation and lowering reaction barriers. This dual "light-heat" mechanism not only mitigates the inefficiency of pure photocatalysis but also eliminates reliance on external heating, maximizing solar energy utilization. The hydrogen-bonding network simultaneously stabilizes intermediates and suppresses side reactions, ensuring high selectivity in H_2O_2 synthesis.

2. Methods

2.1 Materials

Methanol (CH_3OH) was obtained from Beijing Chemical Reagent Company. Hydrochloric acid (HCl) and sulfuric acid (H_2SO_4) were purchased from Tianjin Fuyu Fine Chemical Co., Ltd. Tetrahydrofuran (THF, 99.0%) was purchased from Aladdin. Sodium hydroxide (NaOH), potassium hydroxide (KOH), sodium nitrate ($NaNO_3$), Magnesium nitrate hexahydrate ($Mg(NO_3)_2·6H_2O$), Aluminum nitrate nonahydrate ($Al(NO_3)_3·9H_2O$), potassium titanium oxalate and methyl p-formylbenzoate (98.0%) were purchased from Beijing InnoChem Science & Technology Co., Ltd. Pyrrole (99.0%) was purchased from Adamas-beta. Formaldehyde (99.0%), 5,10,15,20-Tetra(4-carboxyphenyl)porphine (TCPP) and propionic acid (99.0+%) were purchased from Beijing Inokai Science and Technology Company. In this work, all reagents were used as received without further purification. All solutions were prepared with decarbonated deionized water.

2.2 Characterization of the Materials

Photocatalytic reactions were carried out under a Xe lamp (PLS-SXE 300E, Perfect Light) equipped with optical filters (AM 1.5 G, $\lambda \geq 420$ nm), and the irradiance was calibrated using a VLP-2000 laser power meter. Powder X-ray diffraction (XRD) patterns were recorded on a Shimadzu XRD-6000 (3–90° 2θ, 10° min^{-1}). Scanning electron microscopy (SEM) images were obtained on a Hitachi HT7800. UV-visible-near-infrared (UV-vis-NIR) were collected on a Hitachi UV-3900H. Infrared thermography was monitored using a Hikvision E09Pro camera. Electron paramagnetic resonance (EPR) spectra were measured with a Bruker EMX-500 10/12 spectrometer. Photoelectrochemical tests were conducted using a CHI660E workstation.

2.3 Synthesis of TCPP-LDHs

Mg_3Al-NO_3-LDH was prepared by co-precipitation. $Mg(NO_3)_2$ (0.15 M, 200 mL) and $Al(NO_3)_3·9H_2O$ (0.05 M, 200 mL) were simultaneously added with NaOH (2.00 M, 200 mL) into

ISSN: 3007-9640 DOI: https://doi.org/10.70114/acmsr.2025.5.1.P25
NaNO3 solution (1.00 mM, 200 mL) under vigorous stirring while keeping pH = 8. The suspension was aged at room temperature under N_2 for 24 h and washed with decarbonated water.

For TCPP-LDHs, Mg_3Al-NO_3-LDH (0.50 g) was dispersed in a TCPP solution (molar ratio 1:1, pH = 8) and stirred at 80 °C under N_2 for 72 h. The product was washed with water and methanol, and re-dispersed in methanol for storage.

2.4 Photocatalytic H2O2 Production

Photocatalyst (25.0 mg) was dispersed in water (75 mL) in a quartz reactor. O_2 was bubbled (15 min) under stirring to reach adsorption equilibrium, after which the suspension was irradiated with a Xe lamp ($\lambda \geq 420$ nm) in an oil bath. O_2 flow was maintained throughout the reaction. H_2O_2 formation was quantified in triplicate.

2.5 Solar-to-Chemical Conversion Efficiency (SCC)

The SCC efficiency (η_{scc}) for theH_2O_2 production was determined under AM 1.5G simulated sunlight irradiation. The overall irradiation intensity was measured by a laser power meter (VLP-2000). The η_{scc} was determined using the following equation:

$$\eta_{\mathrm{scc}}\,(\%) = \frac{\Delta G_{H_2O_2} \times n_{H_2O_2}}{t \times I} \times 100\%$$

where $\Delta G_{H_2O_2}$, is the free energy for H_2O_2 generation (117 k·mol^{-1}), $n_{H_2O_2}$ is the amount of substance generated by H_2O_2 (mol), t is the irradiation time (1800 s–14400 s), and I is the overall irradiation intensity (l00 mW).

2.6 Photothermal Conversion Efficiency (PTC)

The PTC was measured following literatures. The aqueous solution of Article TCPP-LDH was irradiated by the laser (808 nm, 1 W) until the temperature reached a steady state (~10 min). The PTC value (η) was calculated using eq 1:

$$\eta = \frac{hS(T_{\max} - T_{\mathrm{surr}}) - Q_{\mathrm{dis}}}{I(1 - 10^{-A_{808}})}$$

where T_{max} is the equilibrium temperature and T_{surr} is the ambient temperature of the surrounding. Q_{dis} expresses the rate of heat input due to light absorption by the solvent. I is the laser power (1 W), A_{808} is the absorbance of TCPP-LDH at an excitation wavelength of 808 nm, h is the heat transfer coefficient, and S is the surface area of the container. The value of hS is derived according to eq 2:

$$\tau_{\mathrm{s}} = \frac{m_{\mathrm{D}} C_{\mathrm{P}}}{hS}$$

where τ_s is the sample system time constant. m_D and C_p are the mass and heat capacity of solution, respectively.

3. Results and Discussions

TCPP-LDH nanocomposites were synthesised via the hydrothermal method, with TCPP molecules intercalated between LDH layers to achieve ordered arrangement. The specific preparation process is illustrated in Fig. 1a. The resulting TCPP-LDH composite is depicted in Figure 1b. MaAl-LDH and TCPP-LDH exhibited characteristic (003) and (006) reflections, confirming the successful synthesis of both MgAl-LDH and TCPP-LDH. Crucially, the (003) reflection peak shifted by 7.84° from 11.02°, indicating that the interlayer spacing increased from 0.32 nm to 0.65 nm following TCPP insertion into MgAl-LDH. This expansion can be attributed to the subtraction of the host layer thickness. These characterisation results clearly demonstrate that TCPP molecules adopt a J-type assembly configuration, tilted and inserted into the interlayer spaces of MgAl-LDH (Fig. 1b).

The effect of TCPP intercalation on the morphology of MgAl-LDH was analysed using SEM. As evident from Fig. 1c, TCPP-LDH retains the characteristic plate-like structure of LDH, indicating that intercalation has not altered the fundamental structure of LDH. Furthermore, UV-vis-NIR

ISSN: 3007-9640 DOI: https://doi.org/10.70114/acmsr.2025.5.1.P25
absorption spectra reveals that, compared to TCPP crystals, the absorption wavelength of TCPP-LDH extends towards longer wavelengths, with a new absorption peak appearing at 1000 nm (Fig. 1d). This offers significant advantages for the utilisation of NIR light.

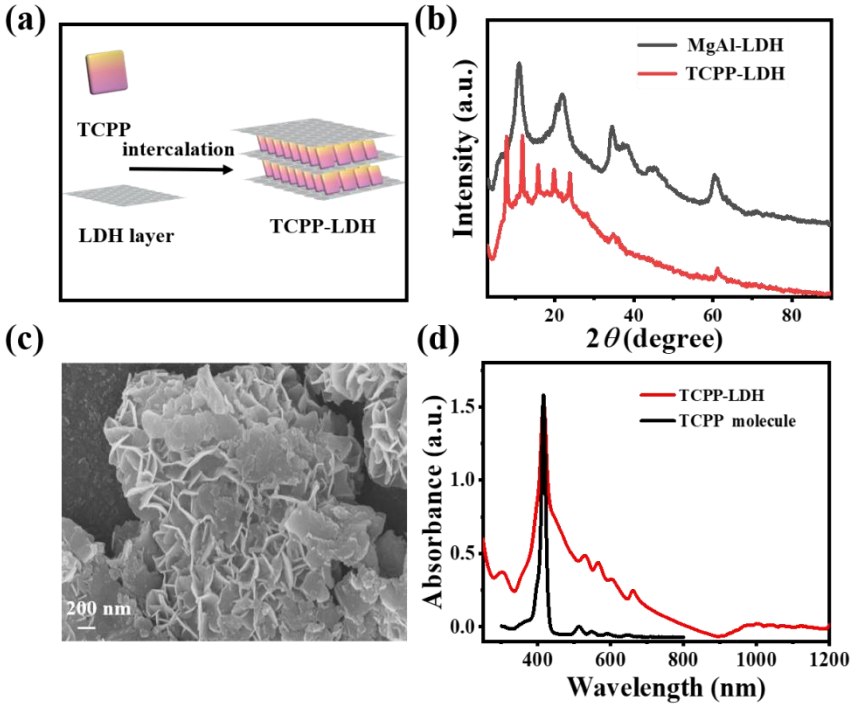

Fig. 1 (a) The schematic illustration for the formation of the TCPP-LDH; (b) XRD patterns; (c)SEM images; (d) UV-vis-NIR absorption spectra.

To further validate the utilisation of NIR absorption, infrared thermal imaging was employed to measure the temperatures of TCPP and TCPP-LDH solutions following irradiation by Xe lamp. Results indicated that the TCPP-LDH system solution reached 346.9 K, whereas the TCPP system solution attained only 308.7 K. The photothermal conversion efficiencies of TCPP-LDH and TCPP were further calculated, with TCPP-LDH achieving 59.8% and TCPP only reaching 19.7%. This further validates that TCPP-LDH can convert NIR light into heat, thereby enabling its full utilisation. Additionally, photocatalytic H_2O_2 generation experiments were conducted under three conditions: an external condensing position temperature of 293.0 K, self-heating of TCPP-LDH without external heat source, and maintaining a temperature of 353.0 K with an external heat source. Results indicate that TCPP-LDH exhibits favourable photocatalytic performance under both self-heating and external heating conditions, yielding cumulative H_2O_2 production of 1.52 mM and 1.60 mM respectively over 4 hours. In contrast, cumulative production at 293.0 K with external condensation maintenance reached only 0.7 mM. To further validate the role of heat in H_2O_2 generation, 2 h catalysis cycles were conducted under xenon lamp irradiation at 278.0 K followed by heating in darkness at 353 K. Alternating this cycle twice yielded cumulative H_2O_2 levels of 0.16 mM under both light irradiation and heating conditions, indicating that light and heat contribute equally to photocatalytic H_2O_2 production.

Calculation results indicate that the adsorption energy of O_2 on TCPP-LDH is –0.493 eV, demonstrating that TCPP-LDH exhibits a tendency for spontaneous adsorption of O_2. Furthermore, to elucidate the mechanism of O_2 involvement in H_2O_2 generation, EPR spectroscopy confirmed that *OOH radicals formed during illumination. This indicates that adsorbed O_2 undergoes photochemical activation to generate *OOH radicals, which subsequently produce H_2O_2. Furthermore, the charge separation efficiency of TCPP-LDH was measured at 61.1%, with a solar-to-chemical energy conversion efficiency (SCC) of 1.6%, further validating its outstanding photocatalytic performance.

ISSN: 3007-9640 DOI: https://doi.org/10.70114/acmsr.2025.5.1.P25

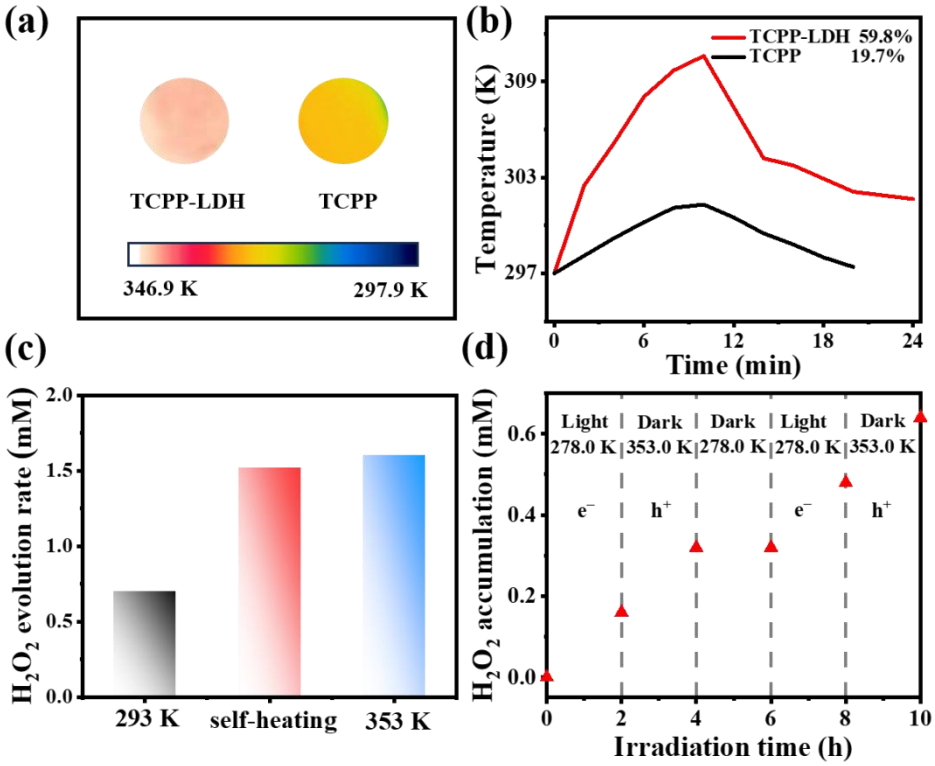

Fig. 2 (a) Infrared thermal images of TCPP-LDH and TCPP molecule suspensions after simulated sunlight irradiation at AM 1.5 G for 40 min; (b) PTC of TCPP-LDH and TCPP; (c) Photocatalytic hydrogen peroxide production performance of TCPP-LDH at 293 K, self-heating and 353 K conditions (Cat. 25.00 mg, 75.0 mL H_2O, 4 h); (d) H_2O_2 production on TCPP-LDH photocatalyst after Xe lamp alternating irradiation and heating of the system every 2 h.

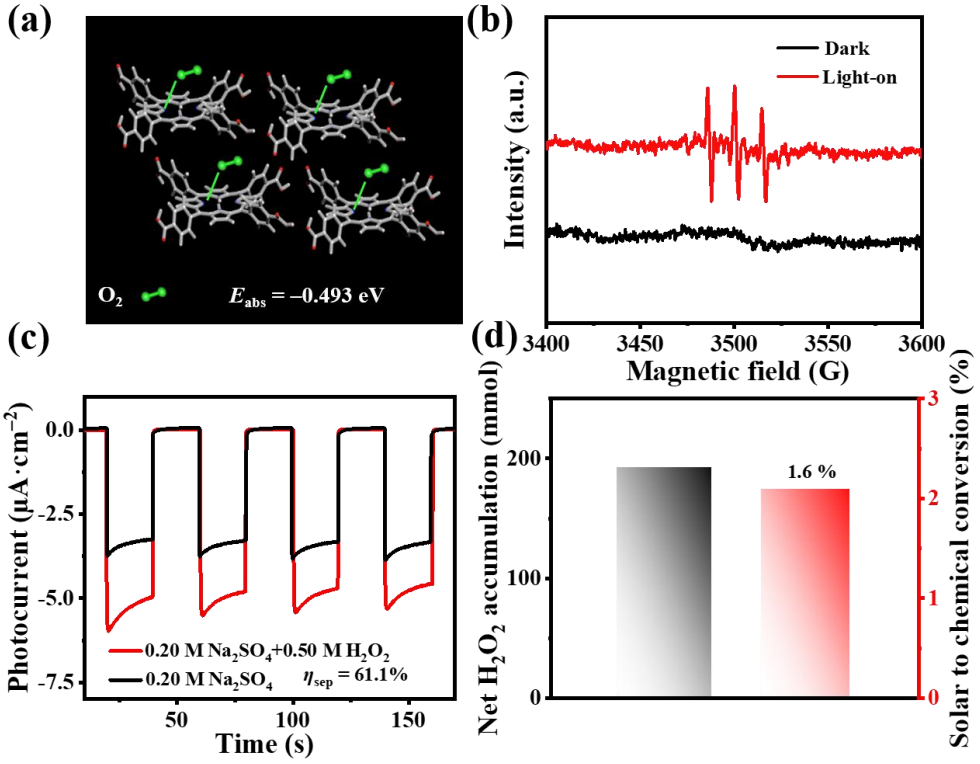

Fig. 3 (a) Oxygen adsorption energies and modeling of TCPP molecules between TCPP-LDH; (b) EPR spectra of TCPP-LDH suspension with 5,5-dimethyl-1-pyrroline N-oxide (DMPO) as the spin-trapping agent; (c) Photocurrent densities and η_{sep} of TCPP-LDH;(d) SCC of TCPP-LDH.

ISSN: 3007-9640 DOI: https://doi.org/10.70114/acmsr.2025.5.1.P25

4. Summary

This study constructed a photothermal coupled catalytic system based on TCPP-LDH. Under two-dimensional confinement, it achieved a transformation of TCPP from H-type to J-type stacking, thereby broadening the spectral response range and significantly enhancing near-infrared absorption and photothermal conversion efficiency. This system achieves dual 'light-heat' dual-drive functionality across the visible to near-infrared spectrum, effectively promoting charge separation and lowering reaction energy barriers. It enables efficient and stable hydrogen peroxide synthesis without sacrificial agents, demonstrating outstanding catalytic activity and energy conversion efficiency. The findings indicate that porphyrin molecular assembly confined within LDH provides novel insights and methodologies for developing green, highly efficient solar-driven hydrogen peroxide production.

Acknowledgements

National Natural Science Foundation of China (22171018 and 22438007).

References

[1] Wang Nan, Ma Shaobo, Zuo Pengjian, et al. Recent Progress of Electrochemical Production of Hydrogen Peroxide by Two-Electron Oxygen Reduction Reaction. Adv. Sci. 2021, 8, 2100076.

[2] Kim Hyoung-il, Choi Yeoseon, Hu Shu, et al. Photocatalytic hydrogen peroxide production by anthraquinone-augmented polymeric carbon nitride. Appl. Catal. B Environ., 2018, 229, 121–129.

[3] Xu Ting, Wang Zhiqiang, Zhang Weiwei, et al. Constructing Photocatalytic Covalent Organic Frameworks with Aliphatic Linkers, J. Am. Chem. Soc. 2024, 146, 20107−20115.

[4] Perry Samuel C., Mavrikis Sotirios, Wang Ling, et al. Future perspectives for the advancement of electrochemical hydrogen peroxide production, Curr. Opin. Electrochem. 2021, 30, 2451–9103.

[5] Wang Tzu-Heng, Chen Min-Jen, Lai YenJung Sean, et al. High-Efficiency Photocatalytic H2O2 Production in a Dual Optical– and Membrane–Fiber System, ACS Sustainable Chem. Eng. 2023, 11, 6465–6473.

[6] Takata Tsuyoshi, Jiang Junzhe, Sakata Yoshihisa, et al. Photocatalytic water splitting with a quantum efficiency of almost unity. Nature. 2020, 581, 411−414.

[7] Han Chuang, Kundu Bidyut Kumar, Liang Yujun, et al. Near-Infrared Light-Driven Photocatalysis with an Emphasis on Two-Photon Excitation: Concepts, Materials, and Applications, Adv. Mater. 2024, 36, 2307759.

[8] Zhong Minling, Sun Yujie, Recent advancements in the molecular design of deep-red to near-infrared light-absorbing photocatalysts, Chem Catalysis, 2024, 4, 100973.

[9] Su Brenden Jing, Foo Joel Jie, Ling Grayson Zhi Sheng, et al. Synergistic redox reactions toward co-production of H2O2 and value-added chemicals: Dual-functional photocatalysis to achieving sustainability. SusMat. 2024, 4, e192.

[10] Zhou Daojin, Li Pengsong, Lin Xiao, et al. Layered double hydroxide-based electrocatalysts for the oxygen evolution reaction: identification and tailoring of active sites and superaerophobic nanoarray electrode assembly, Chem. Soc. Rev., 2021,50, 8790–8817.

[11] Ding Guixiang, Li Chunxue, Ni Yonghao, et al.Layered double hydroxides and their composites as high-performance photocatalysts for CO2 reduction, EES Catal., 2023,1, 369–391.

[12] Rajapakse Manthila, Karki Bhupendra, Abu Usman O., et al. Intercalation as a versatile tool for fabrication, property tuning, and phase transitions in 2D materials, npj 2D Mater Appl, 2021, 5, 30.

[13] Yang Junhao, An Lulu, Wang Shuang, et al. Defects engineering of layered double hydroxide-based electrocatalyst for water splitting, Chinese Journal of Catalysis, 2023, 55, 116–136.

[14] You Hanhui, Wu Dongshuang, Si Duanhui, et al. Monolayer NiIr-Layered Double Hydroxide as a Long-Lived Efficient Oxygen Evolution Catalyst for Seawater Splitting, J. Am. Chem. Soc., 2022, 144, 9254–9263.

ISSN: 3007-9640 DOI: https://doi.org/10.70114/acmsr.2025.5.1.P25
[15] Zhang Yaning, Pan Chengsi, Bian Gaoming, et al. H2O2 generation from O2 and H2O on a near-infrared absorbing porphyrin supramolecular photocatalyst. Nat Energy, 2023, 8, 361–371.

[16] Bodedl Govardhana Babu, Zhu Xunjin, WongWai-Yeung. Recent progress in the development of self-assembled porphyrin derivatives for photocatalytic hydrogen evolution. EnergyChem, 2024, 6, 100138.

[17] Keller Niklas, Calik Mona, Sharapa Dmitry, et al. Enforcing Extended Porphyrin J-Aggregate Stacking in Covalent Organic Frameworks, J. Am. Chem. Soc., 2018, 140, 16544–16552.

[18] Wang Xiaoqing, Jiang Zhiyang, Liang Zhaolun, Discovery of BODIPY J-aggregates with absorption maxima beyond 1000 nm (SWIR) and high photothermal performance. Sci. Adv., 2022, 8, eadd5660.